CAVITATIONAL EROSION RESISTANCE CONSIDERATIONS FOR ALLOY 6082 STATE T651

Ilare BORDEASU[1,2], Brandusa GHIBAN[3], Vasile NAGY[4], Vlad PARAIANU[5], Cristian GHERA[6], Dionisie ISTRATE[7], Alin Mihai DEMIAN[8], Petrisor - Ovidiu ODAGIU[9]

The study presents the results of experimental research on the behaviour and resistance to vibratory cavitation erosion of the structure of aluminum alloy 6082 state 651. The analysis performed on macro and microscopic images shows the degradation mode of the microstructure, and the comparison with alloy 5083 state H111, using the specific parameters of cavitational erosion resistance recommended by ASTM G32-2016 standards, suggests an insignificant difference. Discussions of the plots containing experimental values of the cumulative eroded mass created by cavitational erosion and the related velocities using averaging curves show a behaviour strongly dependent on the nature of the blank, structural homogeneity, mass of intermetallic compounds and mechanical property values.

Keywords: aluminum alloy, cavitational erosion, microstructure, mechanical properties, caverns, erosion rate, lost mass

1. Introduction

The use of aluminum alloys in industrial fields is one of the widest applications, due to their low specific mass and mechanical properties values that

[1] Professor, Romanian Academy of Scientists, Timisoara branch, Timisoara, Romania
[2] Professor, Hydraulics, Hydraulic Machinery and Environmental Engineering, University POLITEHNICA of Bucharest, Romania, ilare.bordeasu@upt.ro
[3] Professor, Dept. of Metallic Materials Science, University POLITEHNICA of Bucharest, Romania, ghiban.brandusa@upb.ro
[4] PhD student, Dept. of Mechanical Machinery Equipment and Transport, University POLITEHNICA of Timisoara, Romania
[5] Lector, Dept. of Hydraulics, Hydraulic Machinery and Environmental Engineering, University POLITEHNICA of Bucharest, Romania
[6] Lector, Dept. of Mechanical Machinery Equipment and Transport, University POLITEHNICA of Timisoara, Romania
[7] PhD student, Dept. of Metallic Materials Science, University POLITEHNICA of Bucharest, Romania, dionisieistrate@yahoo.com
[8] PhD student, Dept. of Metallic Materials Science, University POLITEHNICA of Bucharest, Romania, demianalin96@gmail.com
[9] PhD student, Dept. of Metallic Materials Science, University POLITEHNICA of Bucharest, Romania, odagiuovidiu2017@gmail.com

give resistance to various mechanical and hydrodynamic stresses. For these reasons, they are extensively used in the strength and aerodynamic structure of aircraft, motor vehicles and pleasure craft [1]. As a result of the qualities conferred by the mechanical properties, some of which are comparable in value to steels [2, 3, 4], experimental research started on pure aluminium [5, 6] has been resumed with those on the behaviour and resistance of aluminium-based alloys to cavitation erosion. The aim is for use in parts working under such hydrodynamic conditions, such as: pumps for motor vehicles, rotors of household pumps and propellers of river barges and engines of recreational and fishing boats [5, 7-13]. In step with this research, in the Cavitation Erosion Research Laboratory of the Polytechnic University of Timisoara, using the experience obtained through studies on the increase of the resistance of alloy 5083, in cast and rolled state H111 series, to erosion produced by vibratory cavitations [5], in this study we present the results obtained on alloy 6082 state T651.

2. Material investigated

The material investigated is aluminium alloy 6082 state T651, symbolised AlSi1MgMn, according to EN AW 6082, taken from a 50 mm thick plate. Being anti-corodal, with medium hardness, good corrosion resistance, good mechanical strength and good welding and anodising properties it is intended for mechanically machined parts or welded assemblies such as: boilers, motor boats and recreational sailing boats, digging equipment, truck and trolley frames. In terms of applications in hydraulic equipment, it is mainly used in the housings of hydraulic pumps and other components in the structure of hydraulic drive systems [14, 15].

Tables 1 and table 2 show the chemical composition and the values of the physico-mechanical properties, standard and determined in the specialized laboratory of the Special Materials Expertise Centre of the Politehnica University of Bucharest. The structure is a dendritic one with inclusions of intermetallic compounds, as one can see in Fig.1.

Table 1.

Chemical composition of the experimental alloy

Alloy type	Chemical composition, [%] wt,									
	Si	Fe	Cu	Mn	Mg	Cr	Zn	Ti	Sb	Al
Standard [15]	0.7-1.3	0.5	0.1	0.4-1.0	0.6-1.2	0.25	0.2	0.1	-	rest
Experimental	1.25	0.31	0.09	0.62	0.86	0.17	0.088		0.031	rest

Table 2

Physical and mechanical properties of the experimental alloy

Alloy type	R_m MPa	$R_{p0.2}$ MPa	HB daN/cm^2	A_5 %	ρ g/cm^3	E, GPa	KCU, J

Standard [15]	295-300	240-260	84-89	6-10	2,7	70	
Experimental	226.052	151.71	67	7	2.7	72	25.9

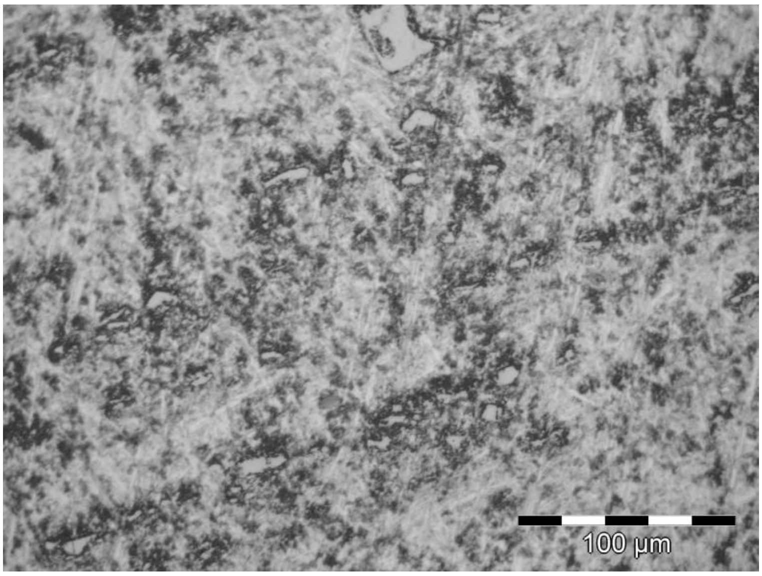

Fig. 1. Microstructural appearance of alloy 6082 specimens (delivery condition)

3. Equipment and research method

The experimental program to investigate the behaviour and resistance to cavitation erosion was carried out on the piezoceramic crystal vibrating apparatus, which is part of the Cavitation Erosion Research Laboratory of the Polytechnic University of Timisoara, using the stationary sample method [5].

The procedure used complies with ASTM G32-2016 [16]. The total duration of the test (broken down into short periods, designed to determine material losses), the analysis of the erosion evolution in the area subjected to cavitations, the processing and interpretation of the recorded data are laboratory routines [11, 17-22], which are not in contradiction with the provisions of ASTM G32-2016. Double distilled water was used as liquid medium, whose temperature was maintained at 22 ± 1^0

For rigour, as required by ASTM G32-2016, three specimens with a standard diameter of 15.8 mm were tested.

According to the test rigors at the start of the cavitating test, the surfaces to be exposed to cavitating were polished to a roughness, Rz =0.2 ÷0.8 µm, fig.2

Fig. 2. Sample surface before exposure to cavitational attack

Throughout the cavitations test, the functional parameters of the apparatus (double vibration amplitude of 50 µm, oscillation frequency of 20 ± 0.1 KHz, electrical power supply of the electronic ultrasound generator of 500 W) were maintained at constant values, due to the fact that the apparatus is connected to a computer, equipped with specially built software [17].

4. Experimental results

Surface degradation morphology

The evolution of cavitational erosion in the surface area and structure is shown by the photographic images in Fig. 3, taken with the Canon Power Shot A 480 camera.

The degree of structural degradation is illustrated by the caverns presented by the images shown in Fig. 4 and 5, obtained by electron microscopy and optics after the completion of the test (165 minutes of exposure to the attack of cavitation).

15 min

60 min

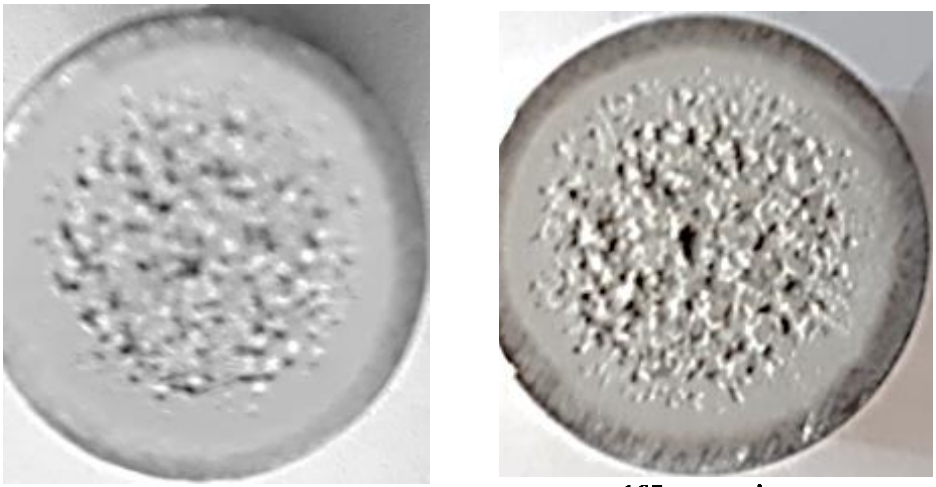

105 min **165 min**

Fig. 3. Macrofractographic images after different cavitational attack durations

The photo images in Fig. 3 show that cavitational erosion of the surface is initiated within the first few minutes, so that within 15 minutes of stressing the asperity peaks are removed and a network of cracks with deformations is generated in the surface, giving the stressed area a sweeping appearance. In the following minutes of stressing, up to 60 minutes, due to the cracks created, small caverns appear which extend into the stressed area due to the breaking of the bonds between the gravels and their expulsion. Continued surface stressing by cavitational microjets leads to the multiplication of caverns, simultaneously with the increase in size (depth and extension in the surface area) of the existing ones. After minute 105, caverns multiply and existing caverns increase more in width and less in depth, due to the impact pressure attenuation mechanism created by the air penetrating the sonotrode compression phase.

Stereomicroscopic analysis, highlighted in Fig. 4, highlights the extent of cavitational attack on the front surface of the specimen. At low magnification power (x8, fig. 4a), a surface with numerous large cavitations, extending over ¾ of the total surface of the specimen, is observed, a sign of an aggressive attack. At higher magnification (x56, Fig. 4b), erosion through caverns is extensive and deep.

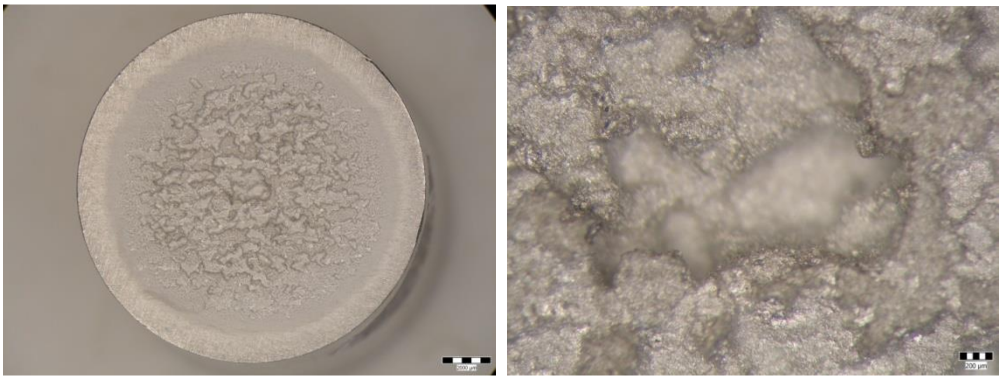

a b

Fig. 4. Stereomicrostructural appearance of experimental specimens after the 165 min cavitational attack (a- x8, b- x56).

The metallographic optical microscope analysis, fig.5, shows that in cross-section the caverns are uneven, with depths varying greatly between them, reaching very large dimensions, about 490 μm.

Scanning electron microscope analysis, fig. 6, shows the fractographic morphology of the cavitational attack. It shows the presence of extensive caverns, in the form of a plateau, together with very shallow caverns, a sign of an intense, aggressive cavitational attack. The fractographic aspect is fragile, through cleavage.

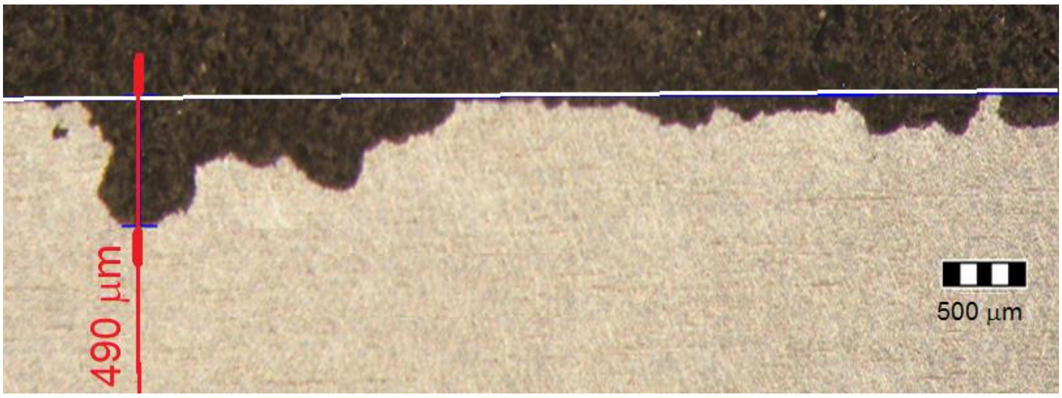

Fig. 5. Metallographic appearance in cross section of specimen subjected to cavitational attack after 165 minutes

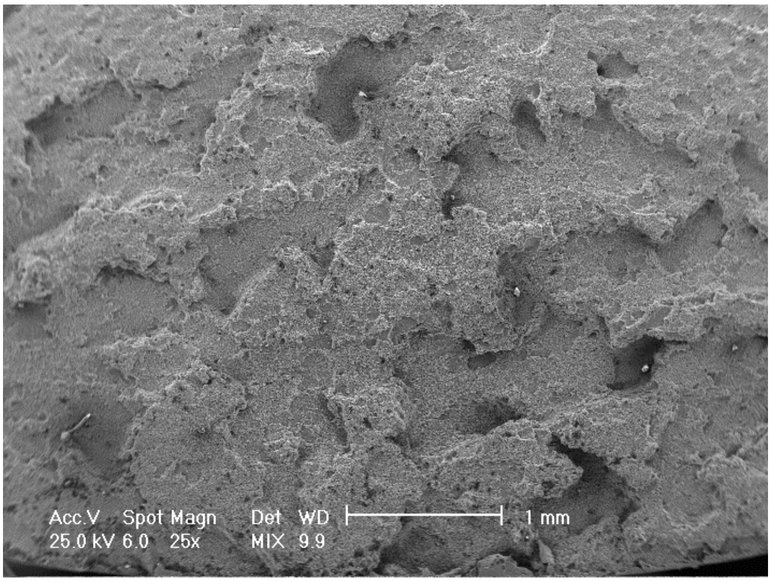

Fig. 6. SEM image of 6082 alloy specimen after cavitational attack, 165 minutes

The complex fractographic analysis carried out on the surfaces subjected to cavitational attack on alloy 6082 samples revealed that the alloy shows numerous caverns, non-uniform on the exposed surface, with sizes ranging from very small, a few microns, up to 490 μm (as shown in Fig. 5). The attack extends over an area of more than 3/4 of the total diameter, and the appearance is brittle through cleavage. The behaviour observed on alloy 6082 in the as-delivered condition is that of a material with extremely low resistance to cavitation corrosion.

Specific curves and parameters

In Figs. 7 and 8 are shown the diagrams used to evaluate the behaviour and resistance to cavitation erosion. They contain the values of the cumulative mass losses and the corresponding mass loss velocities corresponding to the intermediate durations which, summed up, give the total cavitational attack duration (165 minutes).

The mass losses, corresponding to the intermediate periods, are determined with the Zatklady analytical balance which has an accuracy of 10^{-5} grams.

The relationships for determining these mass losses and erosion rates are:

$$M_i = \sum_{i=1}^{i=12} \Delta m_i \tag{1}$$

$$v_i = \frac{\Delta m_i}{\Delta t_i} \tag{2}$$

Where: M_i - means the cumulative mass, in mg

Δm_i – means the mass of material removed by erosion in the time interval Δt_i

i - means the number of the time interval (Δt_1 = 5 min, Δt_2 = 10 min, Δt_3 = Δt_4 =....= Δt_{12} = 15 min)

In these diagrams, specific averaging curves of the experimental values are also plotted, which provide insight into the tendency of the surface structure to behave to cavitational erosion and allow the determination of the values of the parameters Mmax (mass lost through erosion in 165 minutes) and vs (final bearing velocity - stabilization of erosion - at 165 minutes), recommended by ASTM G32-2016 and necessary in the assessment of cavitational resistance [5, 11, 16, 17, 19, 20,].

By the closed red curves, the time intervals in which the mass losses respectively the erosion velocity have high values have been delimited, characterizing the period in which the material yields most to microjet and shock wave stresses. These variations are supported by the photographic (macro) images in Fig. 3.

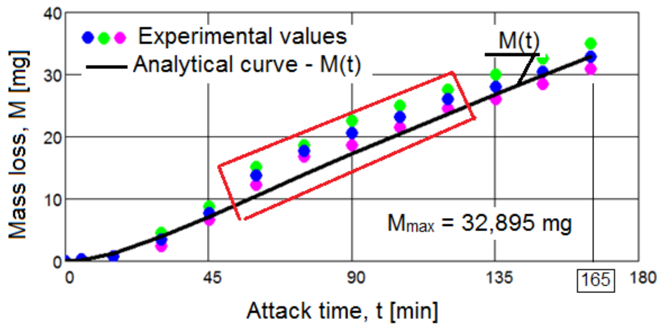

$M(t) = A \cdot t \cdot (1 - e^{-B \cdot t})$; A = 0.2, B = 0.035

Fig. 7. Variation of cumulative mass loss with duration of exposure to cavitations

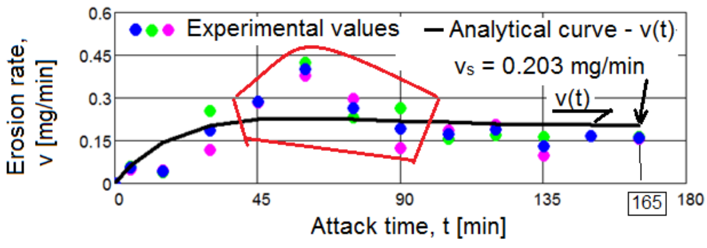

$v(t) = A \cdot (1 - e^{-B \cdot t}) + A \cdot B \cdot t \cdot e^{-B \cdot t}$; A = 0.2, B = 0.035

Fig. 8. Variation of mean erosion rate with duration of exposure to cavitations

The data in Fig. 7 and 8 show the following remarks:

1. the differences between the experimental values, recorded on the three samples, in each intermediate period, are insignificant. The fact that after 90

minutes the differences between the velocity values (fig.8) are almost identical, shows the homogeneity of the structure of the three samples and the running of the experiment with well controlled parameters;

2. the dispersion of the experimental values of the three samples with respect to the averaging curve suggests identical behaviour. Small reversals/differences, over certain time intervals, are natural, given the multitude of factors on which the resistance of the structure to cavitational stress depends;
3. the most significant mass losses occur between 45-120 minutes;
4. significant velocity jumps occur in the 45-90 minute interval;
5. the shape of the approximation/measurement curve of the experimental values of the velocity, with a slight decrease towards the stabilization (final) value, is a specific one for surfaces with average mechanical properties in value (see Table 2), which offer high plasticity but poor resistance to cyclic cavitational stresses [6, 9, 19, 20, 23, 24];
6. the linearly increasing evolution of the M(t) curve, Fig. 7, which leads to the asymptotic decrease of the v(t) curve towards the stabilization value, is determined by the erosive process unfolding with approximately constant losses after 120 minutes of exposure to cavitations.

5. Comparison of results

To evaluate the resistance of the structure of alloy 6082 state T651 to erosion generated by vibratory cavitations, the histogram in Fig. 9 was constructed, using the photographic image and the reference parameters obtained when testing aluminium alloy, semi-finished state 5083 state H111, characterised by the following values of mechanical properties [4]: R_m = 235.367 MPa, $R_{p0.2}$ = 135.78 MPa, HB = 80.1, KCU = 5.3 J.

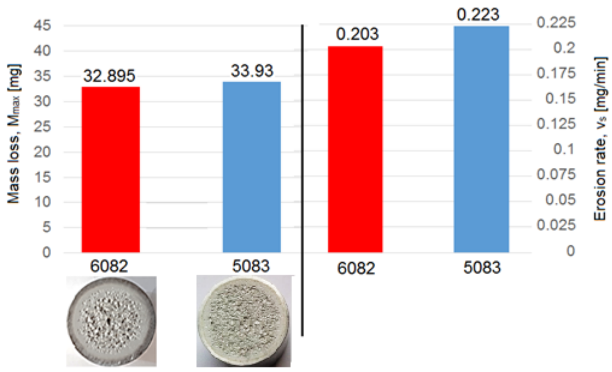

Fig. 9. Histogram of cavitational erosion resistance

The photo images, from below the histogram (fig.9), show the similarity between the size of the caverns and the eroded area. This observation is confirmed by the differences between the values of the M_{max} (about 3%) and vs (about 9.8%) parameters shown in the histogram, recommended by ASTM G32 standards. These values are within the range of deviations accepted for a complex acting process such as cavitational hydrodynamics [5, 19-21]. Practically, these differences are of the order of those recorded between the experimental values of the three samples tested (see Figs. 7 and 8). Therefore, this experiment shows that materials with slightly different structures and with significantly different mechanical properties values, such as those of alloy 6082 compared to alloy 5083 (4 % decrease for R_m, 11.7 % increase for $R_{p0.2}$, 19.55 % decrease for HB hardness and 4.9 times increase for KCU resilience), can have close, even identical, behaviour and resistance to cyclic cavitational microjet stresses. The results reconfirm the complex mechanism, which cannot be dependent only on one single factor characteristic of the material (microstructure or only one of the mechanical properties). These differences can be substantial if technologies and treatments are applied to modify the values of the mechanical properties and the type of microstructure [20, 24-26].

6. Conclusions

The dispersions of the experimental values of the M and v parameters with respect to the averaging curves show that the structure of alloy 6082 state T651 has poor resistance to cavitational erosion, comparable to alloy 5083 state H111.

The shapes of the caverns, their large number and depth are mainly determined by the size of the gravels and the amount of intermetallic compounds, which yield very easily to the impact pressures between the surface and the microjets. The shapes of the caverns and the evolution of the damage, as an extension in the exposed surface area, suggest the need to use treatments to obtain a structure with mechanical properties that can lead to increased resistance to cavitational erosion.

The complex fractographic analysis carried out on surfaces subjected to cavitational attack on alloy 6082 samples revealed that the alloy shows numerous caverns, non-uniform on the exposed surface, with sizes ranging from very small, a few microns, to some that can exceed 490 μm. The attack extends over an area of more than 3/4 of the total diameter, and the appearance is brittle through cleavage. The behaviour observed on alloy 6082 in delivery condition is that of a material with extremely low resistance to cavitation corrosion.

Aknowledgement:

This work has been funded by the European Social Fund from the Sectoral Operational Programme Human Capital 2014-2020, through the Financial Agreement with the title "Training of PhD students and postdoctoral researchers in order to acquire applied research skills - SMART", and Contract no. 13530/16.06.2022 - SMIS code: 153734.

R E F E R E N C E S

[1.] Aluminum catalogue, https://fdocumente.com/document/aluminiu-catalog.html

[2.] Noga, P., Piotrowicz, A., Skrzekut, T., Zwolinski, A., Strzepek, P., Effect of Various Forms of Aluminum 6082 on the Mechanical Properties, Microstructure and Surface Modification of the Profile after Extrusion Process, Materials, Materials 14, 5066. https://doi.org/ 10.3390/ma14175066, 2021

[3.] Tomlinson, W. J., Matthews, S. J., Cavitation erosion of aluminium alloys, Journal of Materials Science volume 29 (1994), Pages.1101–1108, 2004

[4.] Bordeasu, I., Ghera, C., Istrate, D., Salcianu, L., Ghiban, B., Bazavan, D. V., Micu, L. M., Stroita, D. C,, Suta, A., Tomoiaga, I., Luca, A. N, Resistance and Behavior to Cavitation Erosion of Semi-Finished Aluminum Alloy 5083, HIDRAULICA **4**, Pages 17-24, 2021

[5.] Ghera, C., Mitelea, I., Bordeasu, I., Craciunescu, C., Improvement of Cavitation Erosion Resistance of a Low Alloyed Steel 16MnCr5 Through Work Hardening, Metal 2015, Brno, Czech Republic, Jun 03-05, Pages. 661-666, 2015

[6.] Hobbs, J. M., Experience with a 20 – KC Cavitations erosion test, Erosion by Cavitations or Impingement, ASTM STP 408, Atlantic City, USA, 1960

[7.] Tong, Z., Jiao, J., Zhou, W., Yang, Y., Chen, L., Liu, H., Sun, Y., Ren, X., Improvement in cavitation erosion resistance of AA5083 aluminium alloy by laser shock processing, Surface and Coatings Technology, **3** Pages. **77**, 124799, 2019

[8.] Carlton, J., Marine propellers and Propulsion, Elsevier Ltd: Oxford, Great Britane, 2007

[9.] Gottardi, G., Tocci, M., Monte, L., Pola, A., Cavitation erosion behaviour of an innovative aluminium alloy for Hybrid Aluminium Forging, Wear, Volumes 394–395, Pages. 1-10, 2018

[10.] Bordeasu, D., Prostean, O., Hatiegan, C., Contributions to Modeling, Simulation and Controlling of a Pumping System Powered by a Wind Energy Conversion System, Energies, vol.14, Issue, 2, art. Article Number 7696, 2022

[11.] Micu, L.M., Bordeasu, I., Popoviciu, M.O., Popescu, M., Bordeasu, D., Salcianu, L., Influence of volumic heat treatments upon cavitation erosion resistance of duplex X2CrNiMoN 22-5-3 stainless steels, IOP Conference Series-Materials Science and Engineering, (ICAS2014), vol.85, art.number 012019, 2015

[12.] Stroita, D. C., Barglazan, M., Manea, A.S., Balasoiu, V., Double-flux water turbine dynamics, Annals of DAAAM for 2008 and 19th International DAAAM Symposium "Intelligent Manufacturing and Automation: Focus on Next Generation of Intelligent Systems and Solutions", Trnava, 22 October 25 Pages. 1325-1326, 2008

[13.] Luca, A.N., Bordeasu, I., Ghiban, B., Demian, A.M., Cavitation behavior study of the aging heat treated aluminum alloy 7075, 10-Th International Conference of Applied Science (ICAS 2022), Banja-Luka, 26-28 MAY 2022, (in progress)

[14.] Suteu, V., Suteu, Vs., Suteu, M., - technology of maintenance and repair of machines and equipment, Editura Dacia, Cluj-Napoca, 1984 (In Romanian)

[15.] https://color-metal.ro/ro/caracteristici-mecanice-table-benzi-table-groase-placi (in Romanian)

[16.] ***Standard method of vibratory cavitation erosion test, ASTM, Standard G32, 2016

[17.] Bordeasu, I., Monograph of the Cavitation Erosion Research Laboratory of the Polytechnic University of Timisoara (1960-2020) Editura Politehnica, Timişoara, Romania, 2020 (in Romanian), ISBN 978-606-35-0371-9

[18.] Bordeasu, I., Popoviciu, M.O., Mitelea, I., Balasoiu, V., Ghiban, B., Tucu, D., Chemical and mechanical aspects of the cavitation phenomena, REVISTA DE CHIMIE, Issue 12, **58**, Pages. 1300-1304, 2007

[19.] Jurchela, A. D., Research on the erosion produced by vibratory cavitation in stainless steels with constant chromium and variable nickel, Politehnica University of Timisoara, Romania, Doctoral Thesis, 2012, (in Romanian)

[20.] Micu, L.M., The behavior to cavitation erosion of duplex stainles steels, Politehnica University of Timisoara, Romania, Doctoral Thesis, 2017, (in Romanian)

[21.] Bordeasu, I., Mitelea, I., Salcianu, L., Craciunescu, C. M., Cavitation Erosion Mechanisms of Solution Treated X5CrNi18-10 Stainless Steels, JOURNAL OF TRIBOLOGY-TRANSACTIONS OF THE ASME **138** (3) 031102, 2016

[22.] Bordeasu, I., Popoviciu, M.O., Mitelea, I., Salcianu, L., Bordeasu, D., Duma, S.T., Anton, I., Researches upon the cavitation erosion behaviour of austenite steels, IOP Conference Series-Materials Science and Engineering, (ICAS2015), vol.106, art.number 012001, 2016

[23.] Franc, J-P., Kueny, J-L., Karimi, A.T., Fruman, D-H., Fréchou, D., Briançon-Marjollet, L., Billard, J-Y., Belahadji, B., Avellan, F., Jean-Marie, M., La cavitation. Physical mechanisms and industrial aspects, Press Universitaires de Grenoble, Grenoble, France, 1995

[24.] Vadapalli, S., Pathem, U,, Vupplala, V, R, S, N, Chebattina, K. R., Sagari, J,, Corrosion and cavitation erosion properties of sub-micron WC-Co /Cr_3C_2-NiCr multi-layered coating on aluminium substrates, Journal of Metals, Materials and Minerals, Vol. 30, No. 3, Pages. 46-54, 2020

[25.] Lavigne, S., Pougoum, F., Savoie, S., Martinu, L., Klemberg-Sapieha, J.E., Schulz, R., Cavitation erosion behavior of HVOF CaviTec coatings. Wear, **386-387**, Pages. 90-98, 2017

[26.] Song, Q.N., Tong, Y., Xu, N., Sun, S.Y., Li HL, Bao, Y.F., Jiang, Y. F., Wang, Z. B., Qiao, Y. X., Synergistic effect between cavitation erosion and corrosion for various copper alloys in sulphide-containing 3.5% NaCl solutions. Wear, **50**, Pages.11, 203258, 2020